

***Final Draft***  
**of the original manuscript:**

Wiese, B.; Mendis, C.L.; Tolnai, D.; Stark, A.; Schell, N.; Reichel, H.-P.;  
Brueckner, R.; Kainer, K.U.; Hort, N.:

**CaO dissolution during melting and solidification of a Mg–10  
wt.% CaO alloy detected with in situ synchrotron radiation  
diffraction**

In: Journal of Alloys and Compounds (2014) Elsevier

DOI: 10.1016/j.jallcom.2014.08.151

# CaO dissolution during melting and solidification of a Mg-10 wt.% CaO alloy detected with *in situ* synchrotron radiation diffraction

B. Wiese<sup>\*,a</sup>, C.L. Mendis<sup>a</sup>, D. Tolnai<sup>a</sup>, A. Stark<sup>b</sup>, N. Schell<sup>b</sup>, H.-P. Reichel<sup>c</sup>, R. Brückner<sup>c</sup>, K.U. Kainer<sup>a</sup> and N. Hort<sup>a</sup>

<sup>a</sup>MagIC - Magnesium Innovation Centre, Helmholtz-Zentrum Geesthacht, Max-Planck-Straße 1, D-21502 Geesthacht, Germany

<sup>b</sup>Materials Physics, Helmholtz-Zentrum Geesthacht, Max-Planck-Straße 1, D-21502 Geesthacht, Germany

<sup>c</sup>LMpv Leichtmetall - Produktion & Verarbeitung GmbH, Einsteinstraße 4, D-36466 Dermbach, Germany

\*Corresponding author. Tel: +49 4152 871963, Fax: +49 4152 871909, e-mail address: [bjoern.wiese@hzg.de](mailto:bjoern.wiese@hzg.de)

## Abstract

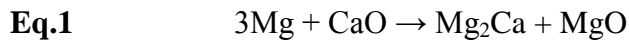
The phase dissolution and evolution during the melting and the solidification of Mg containing 10 wt.% CaO was investigated in the temperature range of 20 - 680 °C. The dissolution of CaO and the formation of Mg<sub>2</sub>Ca were detected with *in situ* synchrotron radiation diffraction. The dissolution of CaO was observed at ~407 °C with the detection of a peak unique to the Mg<sub>2</sub>Ca phase prior to melting of Mg. After the solidification no CaO was detected, and Mg<sub>2</sub>Ca and MgO phases were observed.

**Keywords:** magnesium alloys, solidification, liquid-solid reactions, synchrotron radiation, *in situ* phase evolution

## 1 Introduction

The interactions between Mg and CaO affect the evolution of the microstructure, the mechanical and the corrosion properties of the newly developed ECO (Environment CONscious) Mg alloys [1]. Previous investigations on CaO addition to pure Mg [1-4] and Mg alloys [1,3,5-7] report that the CaO disperses in Mg. These investigations were made on as-cast samples [1-3,6,7] and samples processed via Equal Channel Angular Bulk Mechanical Alloying (ECABMA) subsequently heat treated [5]. After solidification or heat treatment, previous investigation reported, the formation of Laves phase Mg<sub>2</sub>Ca in pure Mg and Al<sub>2</sub>Ca in Mg-Al alloys. According to the Ellingham diagram CaO is more stable than MgO [8], therefore, it is expected that CaO remains unreacted. Kondoh et al. [5] calculated the standard Gibbs free energy for the reaction between pure Mg and CaO using Eq. 1. This thermodynamic hypothesis showed a decrease in the standard Gibbs free energy for the disassociation of CaO and the formation of Mg<sub>2</sub>Ca Laves phase at

low temperatures [5]. Kondoh et al. [5] investigated the solid state reaction between CaO and AZ61 which forms  $\text{Al}_2\text{Ca}$  after mechanical alloying. It is necessary to understand the reactions between Mg and CaO in the solid and liquid states to elucidate the thermodynamics behind the dissolution of CaO. Therefore, it is important to determine which phases are present during heating, in the melt, during solidification; and to follow the dissolution of CaO in pure Mg. This contribution reports the first *in situ* investigation on the dissolution of CaO in Mg during melting and solidification.



## 2 Material and methods

In the present study, the melting- and the solidification behaviour of pure Mg (chips produced by cutting with a machine) mixed with 10 wt.% CaO powder was investigated in the temperature range from room temperature to 680 °C using synchrotron radiation. The 10 wt.% CaO was chosen to identify the dissolution of CaO in Mg and to ensure the volume fraction of pertinent phases remain above the measurement threshold. This allows the detection of the various reactions that occur during in the heating, holding and cooling. The synchrotron radiation diffraction study was conducted at the P07 (High Energy Materials Science) beamline of PETRA III (Deutsches Elektronen-Synchrotron), with a beam energy of 100 keV ( $\lambda = 0.0124$  nm) and a beam cross section of  $1 \times 1$  mm<sup>2</sup>. The samples were heated with the induction coil of a Bähr 805A/D dilatometer modified to prevent interaction of the coil with the X-ray beam. The set-up is isolated with two windows covered with Kapton foils so that the X-ray beam interacts only with the sample [9,10]. The samples were heated in an Ar atmosphere to 500 °C at 100 Kmin<sup>-1</sup>, then to 680 °C at 10 Kmin<sup>-1</sup>. The samples were held at 680 °C for 5 min to ensure melt homogeneity, and then cooled at 10 Kmin<sup>-1</sup> to 500 °C (fully solidified state) before air-cooling to room temperature. The temperature-time-curve was controlled by a S type thermocouple welded on the stainless steel crucible (ME-00029990 120 µl from METTLER-TOLEDO made from stainless steel with a wall thickness of 0.33 mm) containing the pure Mg and CaO powder sample. The two dimensional (2D) diffraction patterns were recorded in transmission geometry at every 6 s with an acquisition time of 3 s with a PerkinElmer XRD 1622 Flatpanel at a sample-to-detector-distance of 1452 mm. This results in a resolution of 10 K for heating at 100 K/min and a resolution of 1 K during heating and cooling at 10 K/min. Consequently the temperature resolution for the heating at 100 K/min is  $\pm 10$  and heating or cooling at 10 K/min is  $\pm 1$ . X-ray line profiles were obtained by azimuthal integration of the 2D diffraction patterns through 360°. For phase identification simulated line profiles were generated with CaRIne 3.1 Crystallography™ with crystal structure data from the Pearsons Crystallography Database [11].

Separate samples for bulk investigations, including scanning electron microscopy (SEM), are produced by casting from pure Mg ingots (99 g) with 10 wt.% CaO (11 g) in a steel crucible using electric furnace (Hornbach Spezialmaschinen GmbH). The melt was held at 680 °C and mixed with CaO powder and held steering for 5 min, and then cast in to steel mould (Ø18x180 mm) preheated to 350 °C.

The specimens for SEM were prepared by grinding with SiC paper to 2500 grit, polishing with a 3 µm

diamond suspension followed by a mixture of 1  $\mu\text{m}$  diamond and OPS<sup>TM</sup> anhydrous suspension. Microstructures were investigated using a Carl ZEISS, ULTRAT M 55 SEM, operating at 15 kV, equipped with an EDAX energy-dispersive X-ray spectrometer (EDXS) and the local compositions determined by point analysis and compositional maps.

### 3 Results and discussion

The SEM investigation of the as-cast Mg-10 wt.% CaO sample shows the formation of the Mg/Mg<sub>2</sub>Ca Laves phase lamellae eutectic in the  $\alpha$ -Mg matrix shown in Fig. 1. As cast bulk samples were used for the SEM investigation as the sample used for the *in situ* synchrotron study could not itself be used for this investigation. The EDXS point analysis (arrowed in Fig. 1a) in this eutectic region shows a Ca content of ~ 8 at.%. The EDX maps of Ca and O show that there is no O enrichment associated with Ca (Fig. 1b, c). However, with EDXS point analysis (Fig. 1d) a small O peak is detected (1.3 at.%). The O content is significantly lower than Ca, thus this phase is unlikely to be pure CaO. Due to the low solid solubility of Ca in Mg (1.34 wt.% / 0.8 at.%) any segregation of Ca that occur within  $\alpha$ -Mg grains during solidification cannot be observed on the EDXS elemental map for Ca.

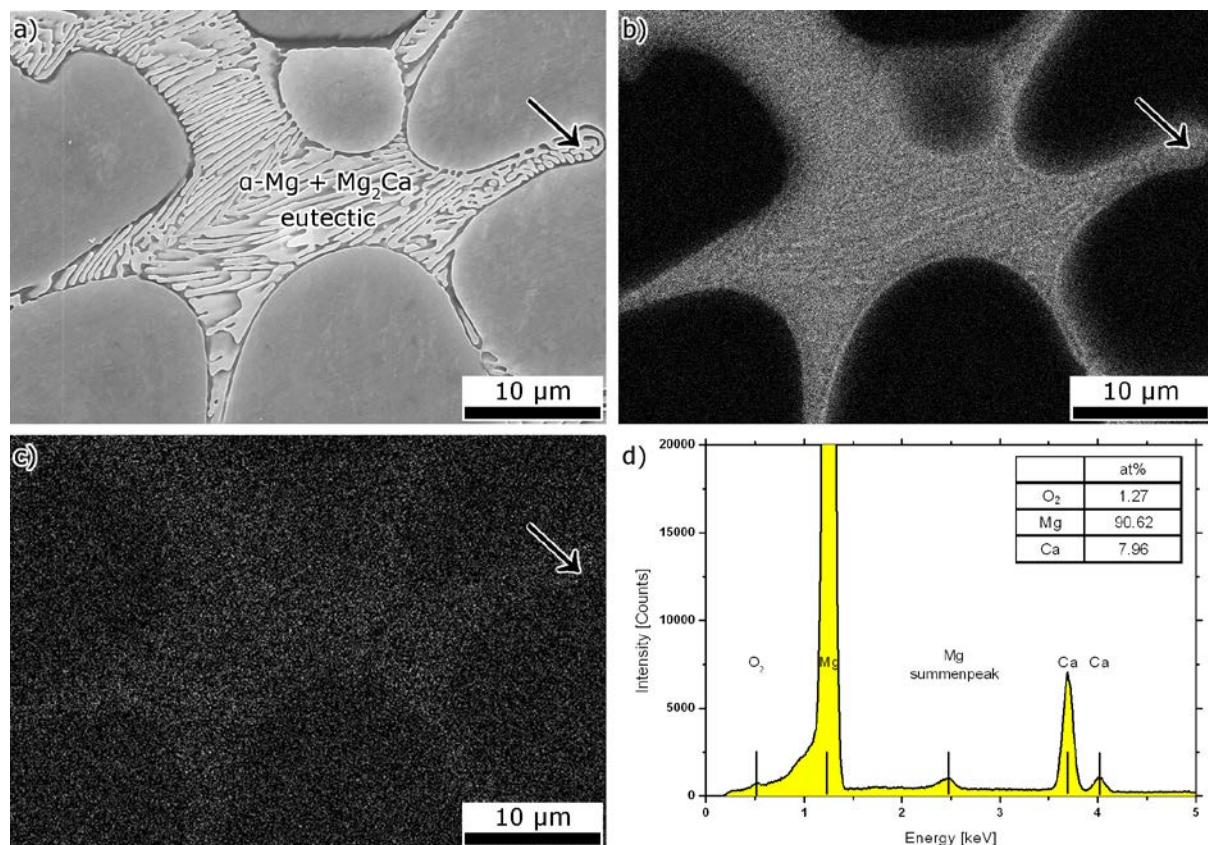


**Fig. 1:** a) Scanning electron micrograph (SEM) of as-cast Mg-10 wt.% CaO alloy. EDXS map of the same area showing b) Ca and c) O. d) EDX spectra recorded from the area as indicated by the arrow.

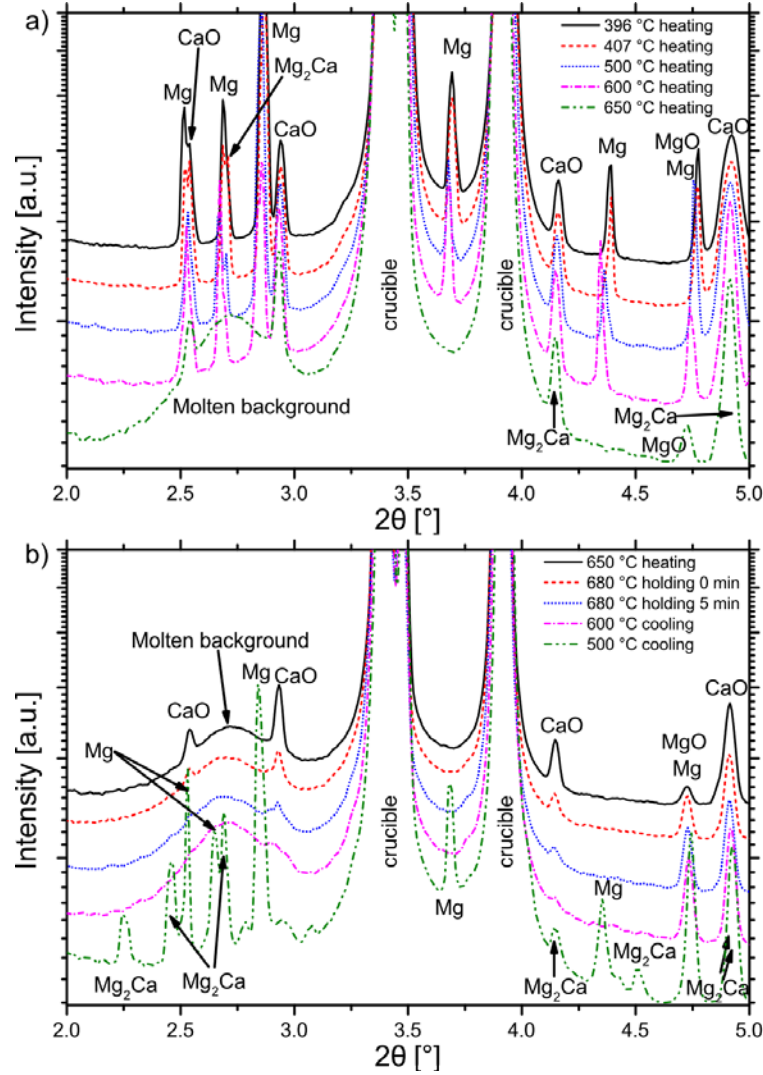


**Fig. 2:** Selected line profiles a) up to the melting stage and b) isothermal holding and solidification with the observed phases indicated.

The X-ray line profiles from the synchrotron investigation show the dissolution of CaO and the formation of  $Mg_2Ca$  and MgO phases during the heating and cooling cycle of the experiment (Fig. 2a). In the powder state the peaks from CaO and Mg are observed. During heating the Mg peaks shifts to smaller angles, as the thermal expansion results in a slight increase in the lattice parameters. The line profile at  $407 \pm 10$  °C shows a double peak at  $\sim 2.7^\circ$  that is comprised of diffraction due to Mg and  $Mg_2Ca$ , as illustrated by the line at 500 °C, Fig. 2a. In the molten state (at  $642 \pm 1$  °C) the intensity of the CaO peaks decrease rapidly while the MgO peak intensity increased. The CaO peaks ( $2.6^\circ$  and  $2.9^\circ$  in  $2\theta$ ) disappear after holding for 5 min at 680 °C but the overlap peaks for  $Mg_2Ca$  and CaO ( $4.14^\circ$  and  $4.91^\circ$  in  $2\theta$ ) remained due to the formation of  $Mg_2Ca$ . To understanding the dissolution of CaO we used the (200) peak from CaO as this peak does not overlap with another phase that were expected in the system (i.e. Mg, MgO or  $Mg_2Ca$  phases). We have not conducted a systematic Rietveld analysis to determine the phase fraction as the investigated sample is not an ideal powder sample. This is related to the slower cooling rate and the grain

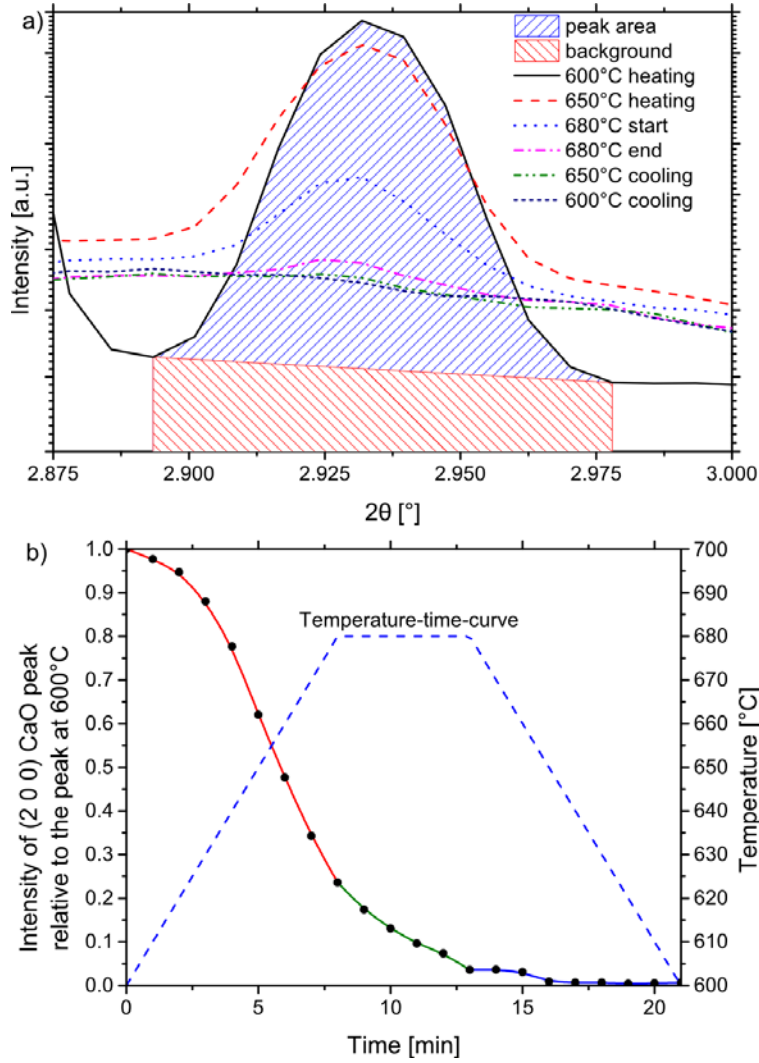


**Fig. 3:** The disassociation of CaO in the Mg a) peak evolution with the intensity change for (200) CaO peak and b) change in the integrated intensity of (200) CaO peak relative to (200) CaO peak at 600 °C.

growth that lead to a non-random distribution of grain orientations. The Fig. 3a shows the main CaO peak (200) and the method used to integrate the peak area. Only the area under the curve without background was used as the integrated peak area. The peak evolution in Fig. 3b shows the change of the integrated peak area of CaO (200) peak during heating, and the dissolution of CaO in the solid and molten Mg is illustrated. In order to follow the dissolution of CaO easily the intergrated peak area of CaO (200) peak was normalised to the CaO (200) peak at 600 °C. The dissolution of CaO starts below the melting temperature of Mg as indicated by the presence of  $Mg_2Ca$ . The reduction of CaO to Ca starts during heating in solid-state before Mg melts. From 600 °C to the melting temperature of Mg (650 °C) the dissolution speed increases, and is expected to be proportional to the solid-state diffusion co-efficient of Ca in Mg. In the molten state (above 650 °C) the dissolution speed of CaO increased significantly, as the diffusion in the liquid Mg is higher than that in the solid Mg. During holding at 680 °C the change in the integrated peak area (dissolution speed) decreases and become constant as shown in Fig. 3b. After cooling to 600 °C the CaO (200) peak decreased to 0.007 that of the CaO (200) peak observed at 600 °C. It is

proposed that in this temperature a reaction layer forms around CaO particles and a critical layer thickness, with high concentration of Mg<sub>2</sub>Ca/MgO. Since this layer can act as a diffusion barrier as it slows down the dissolution of the CaO in Mg. The first set of unique Mg<sub>2</sub>Ca peaks appear during solidification at 505 ± 1 °C, which is below the eutectic temperature of the Mg rich side of the Mg-Ca phase system, 516 °C. The presence of O leads to the ternary phase system Mg-Ca-O which can reduce the eutectic temperature for Mg<sub>2</sub>Ca formation. It is possible that this can explain the reduction of the eutectic temperature for the formation of the Laves phase Mg<sub>2</sub>Ca. However, there is no sufficient information on the Mg-Ca-O system available to conclusively determine this. Another possibility could be the reaction kinetic of the phase formation in the cooling process. During further heating more Mg<sub>2</sub>Ca forms. However, the Mg<sub>2</sub>Ca phase dissolves in liquid Mg above 650 °C as the total content of Ca (3 wt.%) in the alloy is less than the Ca content required for Mg<sub>2</sub>Ca to remain stable above 650 °C.

The formation of Mg<sub>2</sub>Ca Laves phase following solidification is consistent with the previous investigations [2,3,7].

## 4 Conclusions

The investigation on the Mg-10 wt.% CaO system followed the phases evolution during heating, in the molten state and during solidification. The dissolution of CaO in Mg was not expected from Ellingham diagram, but the measurement show the first interaction between Mg and CaO and formation of Mg<sub>2</sub>Ca occurs at 407 ± 1 °C. The dissolution speed increased with the temperature and the dissolution speed significantly increased between 600 °C and 640 °C in the pre-molten state. The reaction in the pre-molten state between Mg and CaO was detected for the first time during an *in situ* investigation. This type of investigation open the possibility to understand the role of CaO in Mg and Mg based alloys. This information can be used for evaluation of thermodynamic calculations and experimental verification of phase diagrams of Mg alloys contenting CaO.

## Acknowledgements

The authors acknowledge the Deutsches Elektronen-Synchrotron for the provision of synchrotron radiation facilities within the framework of the proposal I-20120285 and the Federal Ministry for Economic Affairs and Energy (BMWi) funding for the project MagHyM (20K1107B).

## References

1. Shae K. Kim (2011). Design and Development of High-Performance Eco-Mg Alloys, Magnesium Alloys - Design, Processing and Properties, Frank Czerwinski (Ed.), ISBN: 978-953-307-520-4, InTech, <http://www.intechopen.com/books/magnesium-alloys-design-processing-and-properties>, DOI: 10.5772/13836.

2. S.-H. Ha, J.-K. Lee, H.-H. Jo, S.-B. Jung, and S. K Kim: *Rare Metals*, 2006, vol. 25, pp. 150-154.
3. S.-H. Ha, J.-K. Lee, and S.K. Kim: *Mater. T. JIM.*, 2008, vol. 49, pp. 1081-1083.
4. Y.-B. Huang, I.-S. Chung, B.-S. You, W.-W. Park and B.-H. Cho: *Met. Mater. Int.*, 2004, vol. 10, pp. 7-11.
5. K. Kondoh, J. Fujita, J. Umeda, H. Imai, K. Enami, M. Ohara and T. Igarashi: *Mater. Chem. Phys.*, 2011, vol. 129, pp. 631-640.
6. N. D. Nam, M. Z. Bian, M. Forsyth, M. Seter, M. Tan and K. S. Shin: *Corros. Sci.*, 2012, 64, pp. 263-271.
7. J.-K. Lee, and S.K. Kim: *Mater. T. JIM.*, 2011, vol. 52, pp. 1483-1488.
8. I. Brain and O. Knacke: *Thermochemical Properties of Inorganic Substances*, Springer-Verlag, Berlin, New York, 1973.
9. P. Staron, T. Fischer, T. Lippmann, A. Stark, S. Daneshpour, D. Schnubel, E. Uhlmann, R. Gerstenberger, B. Camin, W. Reimers, E. Eidenberger, H. Clemens, N. Huber, and A. Schreyer: *Adv. Eng. Mat.*, 2011, vol. 13, pp. 658-663.
10. D. Tolnai, C.L. Mendis, A. Stark, G. Szakács, B. Wiese, K.U. Kainer and N. Hort: *Mater. Lett.*, 2013, vol. 102-103, pp. 62-64.
11. P. Villars and K. Cenzual: *Pearson's Crystal Data – Crystal Structure Database for Inorganic Compounds (on CD-ROM)*, Materials Park, Ohio, USA, 2012.